PHYSICAL REVIEW D **86,** 065007 (2012)

Entanglement renormalization and holography

Brian Swingle*

Department of Physics, Massachusetts Institute of Technology, Cambridge, Massachusetts 02139, USA and Department of Physics, Harvard University, Cambridge, Massachusetts 02138, USA

(Received 13 September 2011; published 5 September 2012)

We show how recent progress in real space renormalization group methods can be used to define a generalized notion of holography inspired by holographic dualities in quantum gravity. The generalization is based upon organizing information in a quantum state in terms of scale and defining a higher-dimensional geometry from this structure. While states with a finite correlation length typically give simple geometries, the state at a quantum critical point gives a discrete version of anti-de Sitter space. Some finite temperature quantum states include black hole-like objects. The gross features of equal time correlation functions are also reproduced.

DOI: 10.1103/PhysRevD.86.065007 PACS numbers: 03.65.Ud, 03.67.Mn, 04.70.Dy, 64.60.ae

I. INTRODUCTION

Hilbert space, the mathematical representation of possible states of a quantum system, is exponentially large when the system is a macroscopic piece of quantum matter. Understanding the structure of such an exponentially large many-body Hilbert space is one of the great challenges of modern quantum physics. The traditional theory of symmetry breaking reduces this overwhelming amount of information to three key quantities: the energy (or Hamiltonian), the symmetry of the Hamiltonian, and the pattern of symmetry breaking. However, the existence of exotic phases of matter not characterized by broken symmetry, as in the fractional quantum Hall effect [1–3], demonstrates the need for a more general theory. Such systems are distinguished by the presence of long-range entanglement in the ground state [4,5], suggesting that important information is encoded in the spatial structure of entanglement. Here we show how such a ''pattern'' of entanglement can be defined and visualized using the geometry of an emergent holographic dimension. This picture connects two new tools in many-body physics: entanglement renormalization and holographic gauge/gravity duality.

Entanglement renormalization [6] is a combination of real space renormalization group techniques and ideas from quantum information science that grew out of attempts to describe quantum critical points. The key message of entanglement renormalization is that the removal of local entanglement is essential for defining a proper real space renormalization group transformation for quantum states. This realization has permitted a compact description of some quantum critical points [7,8]. Holographic gauge/gravity duality [9–11] is the proposal that certain quantum field theories without gravity are dual to theories of quantum gravity in a curved higher-dimensional ''bulk'' geometry. Real space renormalization is also important in the holographic framework [12–15], thus hinting at a possible connection between holography and entanglement renormalization. We will begin with entanglement renormalization and build up to the full holographic picture.

II. MANY-BODY ENTANGLEMENT

We are interested in quantifying entanglement in many-body systems, and we will use the entanglement entropy $S(A)$ of a subregion A as a measure of entanglement. Entanglement entropy is defined as $S(A) = -\mathrm{Tr}_A(\rho_A \ln \rho_A)$ where $\rho_A = \mathrm{tr}_{\bar{A}}(\rho)$ is the state of A ($\bar{A}$ is the complement of A). If the global state ρ is pure then we have $S(A) = S(\bar{A})$ and nonzero $S(A)$ implies that A is entangled with its environment $\bar{A}$. Considerable evidence suggests that in most cases the entropy satisfies a boundary law: $S(A)$ is proportional to the size of the boundary ∂A [16]. This relationship is violated weakly in one-dimensional critical systems where the entropy scales as $\frac{c}{3}\ln(L)$ with L the length of the region and c the central charge [17,18]. Random quantum states drawn from the Haar measure strongly violate the boundary law with $S(A)$ proportional to the size of A [19]. Together this information suggests that quantum ground states exist in a very special corner of the many-body Hilbert space.

Thus we would like to understand in more detail how to characterize the special ''corner'' of Hilbert space where quantum ground states live. The universality of the boundary law suggests that it follows from an equally universal structure of local quantum systems: the renormalization group. Let r denote the length scale at which we study our system. We partition the degrees of freedom into groups equally spaced in $\log r$ with measure dr/r [20]. Degrees of freedom at each scale can be entangled with A, which we take to have linear size L in d spatial dimensions.

Locality suggests that the contribution to the entropy of A from scale r should be proportional to the size of the boundary ∂A in units of the coarse-grained scale r. The number of entangled degrees of freedom at scale r is also

*brians@physics.harvard.edu

proportional to the measure dr/r. The infinitesimal entropy contribution is thus

$$dS(r) \sim \left(\frac{L}{r}\right)^{d-1} \frac{dr}{r}. \tag{1}$$

The total entanglement entropy is obtained by integrating this formula from the ultraviolet (UV) cutoff to some larger infrared (IR) length $\min(L, \xi_E)$. ξ_E is the length scale beyond which there is no entanglement in the quantum state, so we integrate until the quantum state has no more entanglement or until the region has been coarse-grained to a point. The integral gives a boundary law for $d > 1$,

$$S_{d>1} \sim \left(\frac{L}{\epsilon}\right)^{d-1} - \left(\frac{L}{\min(\xi_E, L)}\right)^{d-1}, \tag{2}$$

and a logarithm for gapless systems ($\xi_E \to \infty$) in $d = 1$,

$$S_{d=1} \sim \ln\left(\frac{\min(\xi_E, L)}{\epsilon}\right). \tag{3}$$

The usefulness of this simple estimate is considerable. It unifies the boundary law and its apparent violations in one dimension and connects the structure of entanglement to the renormalization group, a well-studied structure in quantum matter. As we will see, it also provides the foundation for a simple geometrical picture correlation and entanglement in local quantum systems. In many ways, it is concretely realized by holographic duality, but before turning to holography proper we will give these ideas more concrete form in the guise of a lattice spin model.

III. LATTICE IMPLEMENTATION

We now realize the above scaling argument in a lattice system where entanglement renormalization can be carried out numerically [7]. We study the quantum Ising model in one spatial dimension with Hamiltonian

$$H = -J\sum_{\langle ij\rangle} \sigma_i^z \sigma_j^z - gJ\sum_i \sigma_i^x, \tag{4}$$

where J sets the overall energy scale and g is a dimensionless parameter we can tune. The Hamiltonian consists of two competing pieces, and this competition gives rise to a quantum phase transition at $g = 1$ between an ordered ferromagnetic phase ($g < 1$) and a disordered paramagnetic phase ($g > 1$).

Following the prescription of entanglement renormalization, we implement a renormalization group transformation on the Ising ground state using unitary operators, called disentanglers, to remove local entanglement and isometries to coarse grain as shown in Fig. 1. Note that information can be lost during the coarse graining steps since the isometries typically contain projectors. The resulting network of unitary and isometric tensors approximately encodes the ground state wave function using a multilayered structure [21]. Each layer, indexed by $m = 0, 1, \ldots,$ corresponds to a different length scale $\log(r_m/a) = m\log 2$, so that $m = 0$ is the lattice scale with $r = a$. Considering the extra index m we see that the quantum state is effectively extended into an emergent dimension representing renormalization group scale.

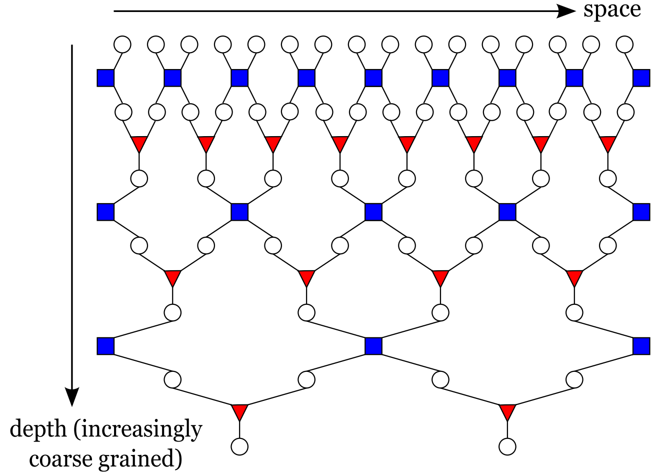

FIG. 1 (color online). The tensor network structure of entanglement renormalization. Circles are lattice sites at various coarse-grained scales. Squares with four lines are unitary disentanglers and triangles with three lines are isometric coarse graining transformations. The network shown here represents a $2 \to 1$ coarse graining scheme and has a characteristic fractal structure. In principle, each tensor can be different, but requiring translation and scale invariance provides strong constraints.

Inspired by holography and our scaling argument above, we will define a discrete geometry from the entanglement structure of the quantum state. We view each site in the network as a cell filling out a higher-dimensional "bulk". The size of each cell is defined to be proportional to the entanglement entropy S(site) of the site in the cell. The connectivity of the geometry is determined by the wiring of the quantum circuit implementing renormalization. Disentanglers that remove more entanglement lead to stronger geometrical connections because they can create or remove more entropy. The geometry ends whenever the coarse-grained state completely factorizes.

To compute the entropy of a block of sites in the original UV lattice, we must know the reduced density matrix of the block. The causal cone [21] of a block of sites in the UV is defined as the set of sites, disentanglers, and isometries that can affect the chosen block. The causal cone should not be confused with ordinary causality in time. For the causal cone of a large block, the number of sites in a given layer shrinks exponentially with layer index, but note that for a small block, the causal cone will fluctuate around a few sites.

We start with the density matrix for a small number of sites deep in the causal cone of the block. The goal is to reach the UV by following the renormalization group flow backwards. This is possible because we have recorded the entire renormalization "history" of the state in the network. More properly, the tensor network defines a large

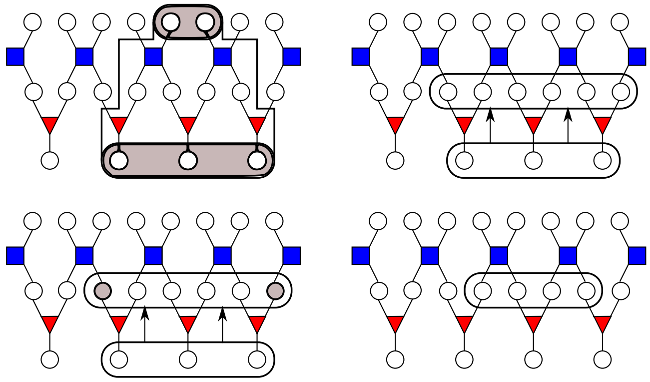

FIG. 2 (color online). (Upper left) A piece of the causal cone of a small block. (Upper right) Reversing the flow to proceed from three sites to six sites. (Lower left) Shaded sites are outside the causal cone of the two-site block and can be traced out. (Lower right) Four sites remain and we can now apply the next layer of disentanglers to reach the two-site block of interest.

variational class of states for which the entanglement entropy can be computed by "reversing the flow" [21].

Thus we reverse the isometries and disentanglers to produce the density matrix of a larger number of sites at a less coarse-grained scale. Any site at the new scale which is not in the causal cone of the block of interest can immediately be traced out as shown in Fig. 2. Tracing out a site can increase the entropy of the remainder, but the increase is no more than the entropy of the traced out site. This procedure is repeated until the UV is reached. Looking at the whole process, sites that are traced out occur on the outside boundary of the causal cone and form a curve in the bulk geometry. The length of this curve is by definition the sum of the entropies of all the traced out sites. Thus the length of a curve in the bulk provides an upper bound for the entropy of a block in the UV.

This entropy calculation is a complicated process, but we can extract at least two general lessons. First, the intuitive picture of distinct entropy contributions from each scale is realized concretely. Second, subadditivity of the entropy permits us to give a discrete geometric upper bound for the entropy of a block of sites in the UV. In fact, this curve is a holographic screen that hides information [22,23]. We emphasize that the boundary of the causal cone is a minimal curve since it represents the minimal number of sites that must be traced out. As an aside, when the number of local degrees of freedom is large, similar to a thermodynamic limit, subadditivity is expected to be replaced by approximate additivity.

IV. GEOMETRY FROM ENTANGLEMENT

What geometries do these definitions give for the Ising model? In the large g limit, the Ising Hamiltonian is dominated by the transverse field, and the ground state is a product state. Each site is in a pure state and we find no geometry. Away from large g, the system possesses a finite correlation length. The size of our cells is initially nonzero due to the presence of entanglement. However, after a finite number of coarse-graining steps any short range entanglement will be removed. At this factorization scale, which is ξ_E, the coarse-grained quantum state factorizes, and the geometry ends. The entanglement entropy of a block in the UV lattice receives contributions from a finite range of scales corresponding to a minimal curve hanging down from the UV to the factorization scale.

The geometrical picture becomes more interesting at the quantum critical point $g = 1$. Scale invariance forces each coarse-grained layer to be identical, and the geometry continues forever. It has been verified numerically that each coarse-grained layer in the network gives an equivalent contribution to the entropy of a block, which means that the entropy is actually proportional to the length of a minimal curve [7]. Because of the fractal nature of the network, the distance between points also shrinks after each coarse graining. Entanglement renormalization is crucial for this result since we would have to keep many more states in the local Hilbert space without it.

The discrete geometry that appears at the critical point is nothing but a discrete version of anti-de Sitter space (AdS), by which we mean a graph whose connectivity mimics the geometry of AdS. The smooth version of two-dimensional anti-de Sitter space has the metric

$$ds^2 = R^2\left(\frac{dr^2 + dx^2}{r^2}\right) = R^2\left(dw^2 + \frac{\exp(-2w)}{a^2}dx^2\right), \quad (5)$$

where R is some constant and $w = \log(r/a)$. In the lattice setup w is simply the number of renormalization group (RG) transformations and corresponds to the layer index. The parameter R controls how big the geometry is and hence should roughly correspond to the amount of local entanglement. Larger R means larger entanglement, for example, at one-dimensional critical points R would be expected to increase with the central charge c. Indeed, it is an old result in the holographic literature that R is actually proportional to c. In the context of our lattice model, R is a measure of the strength of disentanglers and hence the entropy of local sites.

Let us briefly elaborate on what it means for a graph to emulate a continuous space. To begin, let us consider two curves, γ_1 and γ_2, in the geometry of Eq. (5). We take $\gamma_1 = \{(x(t) = x_0 t, r(t) = r_0) | t \in [0, 1]\}$ and $\gamma_2 = \{(x(t) = x_0 \cos(\pi t), x_0 \sin(\pi t)) | t \in [0, 1]\}$; γ_1 is a line at fixed r while γ_2 is a geodesic connecting $(x_0, 0)$ to $(-x_0, 0)$. We can compute the lengths of these two curves to find $|\gamma_1| = R(x_0/r_0)$ and $|\gamma_2| = 2R\ln(x_0/a)$, where a is a cutoff at small r. Now we can compare these two lengths to corresponding lengths using the graph distance in our discrete version of AdS. A straight-line curve at the lattice scale ($r = a$) of x_0/a units will correspond to a length of $R(x_0/a)$ if we use R as the length per bond. The corresponding curve at RG step w_0 has length $R(x_0/a)e^{-w_0}$ since e^{w_0} sites have been grouped into a single site after w_0 RG steps, but this is nothing but $R(x_0/r_0)$ in agreement with the continuous result. Finally, let us consider the analog of the geodesic curve. The minimal lattice path connecting two points x_0/a units apart at the lattice scale ($r = a$) is, up to terms of order one, given by a path which moves straight down in the RG direction until the two sites are side by side. The length of this path, again up to order-one terms, is given by $2R\ln(x_0/a)$, where $\ln(x_0/a)$ is the number of RG steps necessary to bring the sites adjacent and the factor of 2 comes from the two sides of the path. This again agrees with the continuum result up to terms of order one.

We have just shown that various interesting curves have approximately the same length in our discrete AdS geometry as in the true continuous AdS space. This is valuable intuition, but can we say anything more general about why these structures are related? A useful point of contact is provided by random walks and diffusion processes. For example, a random walk on the infinite square lattice can be modeled, at long times, as a diffusion process controlled by the Laplacian of the continuous plane. This is because the low-lying eigenvalues of the graph Laplacian, which controls the random walk, are given by the eigenvalues of the usual continuous Laplacian i.e., $\cos(q_x a) + \cos(q_y a) \to 2 - \frac{a^2}{2}(q_x^2 + q_y^2)$ for small q (wave vector). Something similar happens for the discrete AdS graph we are considering.

Consider a scheme in d-spatial dimensions where k^d sites are renormalized into a single site and where sites at a given RG level are connected in a d-dimensional hypercubic lattice. The graph Laplacian $\triangle_G$ on a graph $G = (V, E)$ acts on functions $f\colon V \to R$ and is defined by

$$\triangle_G f(v) = f(v) - \frac{1}{n_E(v)} \sum_{v', \langle vv'\rangle \in E} f(v'), \tag{6}$$

where $n_E(v)$ is the number of edges leaving vertex v. If we restrict our discrete AdS graph to a given RG scale, then we will recover the usual d-dimensional flat space Laplacian as the long wavelength limit of the graph Laplacian on the hypercubic lattice. However, we must also consider the RG direction. As a simple example, let us search for zero modes of the graph Laplacian depending upon only the RG direction. Let $f(n)$ be the value of the zero mode f at RG step n. We have

$$0 = (\triangle f)(n) = f(n) - \frac{k^d f(n-1) + f(n+1) + 2df(n)}{1 + 2d + k^d}, \tag{7}$$

which may be solved by setting $f(n) = \alpha^n$. This substitution gives the algebraic equation

$$0 = \alpha^2 - (1 + k^d)\alpha + k^d, \tag{8}$$

which has solutions

$$\alpha = 1, \qquad k^d. \tag{9}$$

To compare with the continuum case, consider the continuous Laplacian

$$\triangle_{\mathrm{AdS}} f = \frac{1}{\sqrt{g}} \partial_\mu (\sqrt{g} g^{\mu\nu} \partial_\nu f), \tag{10}$$

with $g_{rr} = (R/r)^2$ and $g_{ii} = (R/r)^2$ for $i = 1, \ldots, d$ the metric components, $g^{\mu\nu}$ the inverse metric, and with $g = \det(g_{\mu\nu})$ the metric determinant. If we look for zero-mode solutions where f depends only on r then we must solve

$$0 = r^{d+1} \partial_r (r^{-(d+1)} r^2 \partial_r f). \tag{11}$$

Assuming that $f = r^\Delta$ we have

$$\Delta(\Delta - d) = 0. \tag{12}$$

Now in the discrete graph setting, $n \to n + 1$ corresponds to rescaling lengths by a factor of $1/k$ and hence we should set $r \sim k^n$ to compare with the continuum result, but then we immediately see that the two discrete zero modes going like 1^n and k^{dn} perfectly match the continuum zero modes going like r^0 and r^d. This hopefully gives some idea of the sense in which a graph can replicate the geometry of a continuous space.

Having now extensively motivated our idea of associating the discrete graph generated by entanglement renormalization with a continuous geometry (like AdS in the critical case), let us recapitulate our correspondence. The collection of unitaries and isometries that generate the quantum ground state $|\psi\rangle$ from an unentangled state $|\psi_0\rangle$ forms a quantum circuit that we call U_{RG}. Our proposal here is to associate U_{RG} with a discrete geometrical space that encodes the local structure of entanglement produced by the circuit. Clearly U_{RG} contains more information than this simple geometric data, but we argue that this is already a very useful picture of the action of U_{RG}. Before exploring the consequences of this association in more detail, let us explore a few more examples of this correspondence, namely what happens at finite temperature.

V. FINITE TEMPERATURE AND CORRELATION FUNCTIONS

Extending our analysis to finite temperatures requires a shift in thinking due to the presence of classical correlations in addition to quantum entanglement. ‘‘Entanglement’’ entropy now has an extensive component due to thermal effects, hence the quotation marks. However, the mutual information $I(A, B) = S(A) + S(B) - S(AB)$ between two regions A and B subtracts out this extensive piece and obeys a boundary law at finite temperature [24]. This boundary law indicates that our previous renormalization group argument for the locality of entanglement still applies to entanglement and classical correlation between spatial regions at finite temperature. The appropriate generalization of entanglement renormalization is thus still useful in removing local entanglement and correlations. To be precise, we employ a doubled quantum circuit to renormalize the thermal density matrix $\rho(T)$, that is we write $\rho(T) = U_{\mathrm{RG}}(T)\rho_0 U_{\mathrm{RG}}(T)^{-1}$ instead of $|\psi\rangle = U_{\mathrm{RG}}(0)|\psi_0\rangle$. The coarse-grained Hilbert space will typically grow if we insist on keeping all eigenvalues of the reduced density matrix of a block up to some fixed cutoff.

The place where finite temperature has the most profound impact is at the quantum critical point. There we initially find a region of discrete AdS geometry for energy scales much greater than the temperature. However, the temperature grows as we renormalize since it represents a relevant perturbation of the critical point (finite size in the imaginary time direction). Thermal effects gradually become important, and the size of coarse-grained sites must begin to grow to incorporate thermalized degrees of freedom. Note that for our model, there is no hydrodynamic behavior for conserved currents, but the order parameter displays low energy "quantum relaxational" dynamics [25]. What would be the "hydrodynamic" scale is characterized by a renormalized temperature greater than the energy scale of interest but still less than the lattice scale. If the temperature continues to grow under further renormalization then it may exceed even the lattice scale, a result familiar from the real space renormalization group of the classical one-dimensional Ising model.

At this final scale the reduced density matrix of any site is proportional to the identity, and the coarse-grained density matrix completely factorizes. We interpret this situation as corresponding to a black hole horizon for three reasons. First, the geometry ends from the point of view of an observer "hovering" at fixed scale. Second, the completely mixed state is like an infinite temperature state, and the local temperature measured by a hovering observer diverges at simple black hole horizons. Third, the final layer has nonzero size because the coarse-grained sites are in mixed states. In particular, the entropy of a large block in the UV now consists of two pieces: the usual boundary contribution plus an extensive piece due to the horizon.

Having accumulated an interesting set of RG circuits and discrete geometries, let us investigate some of the other physical consequences of our proposal. Equal time correlation functions are quite interesting when viewed geometrically. Two local operators, $\mathcal{O}(x)$ and $\mathcal{O}(y)$, can be correlated if the sites, x and y, at which they are inserted have overlapping causal cones. The causal cone of a single site is a "thickened" line in the bulk geometry with a width of a few sites. Consider a simple gapped system. Sites separated by less than a correlation length have overlapping causal cones, but distant sites have causal cones that end at the factorization scale before touching. Thus distant sites, that is sites with $|x - y| \gg \xi_E$, cannot be correlated, a sharp cutoff version of the exponential decay of correlations in a gapped phase.

In the case of a critical geometry, the causal cones of distant sites always touch. For primary operators $\mathcal{O}_\Delta$, which have a simple scaling behavior under renormalization, the correlation functions have an additional geometrical interpretation. Scale invariance demands that $\langle \mathcal{O}_\Delta(x)\mathcal{O}_\Delta(y)\rangle = |x-y|^{-2\Delta}$ with Δ the scaling dimension. From our geometric perspective the correlator of two primary operators separated by $|x-y|$ is proportional to $\exp(-\Delta\ell)$, where Δ is the operator dimension and $\ell \sim 2\log|x-y|$ is the length of a minimal curve connecting them. This is because we can compute the correlator by systematically moving the operators down through the network and because they are primaries they merely acquire a scale factor λ^Δ after each coarse-graining step. λ is determined by the renormalization scheme e.g., $\lambda = 1/k$ for a $k \to 1$ site scheme but Δ is universal. Each operator must be renormalized roughly $\log_k(|x-y|/a)$ times (the minimal number of steps in the extended geometry necessary to connect the two operators) with each renormalization bringing a factor of $k^{-\Delta}$ for each operator. Putting all the factors together gives for $\langle \mathcal{O}_\Delta(x)\mathcal{O}_\Delta(y)\rangle$ roughly

$$\exp\left[-2(\Delta \log k)\left(\frac{\log|x-y|}{\log k}\right)\right] \sim |x-y|^{-2\Delta}. \tag{13}$$

At finite temperature, the horizon is a source of decaying correlations because the causal cones of distant sites can end at the horizon before touching. In each case, the structure of correlation functions is determined by the geometry.

Although the role of the geometry is already clear at the level of two-point functions, it is also instructive to study the structure of higher-point functions. For critical points which possess conformal symmetry (e.g., the Ising critical point we have been using as an example) the three-point function of primary fields is also totally constrained by conformal invariance. For operators O_i of dimension Δ_i the result is

$$\langle O_1(r_1)O_2(r_2)O_3(r_3)\rangle \sim \frac{1}{r_{12}^{\delta_{12}}}\frac{1}{r_{23}^{\delta_{23}}}\frac{1}{r_{13}^{\delta_{13}}}, \tag{14}$$

with $r_{ij} = |r_i - r_j|$ and $\delta_{ij} = \Delta_i + \Delta_j - \Delta_{k\neq i,j}$. With this result in mind, let us see what structure entanglement renormalization predicts for higher-point correlation functions.

Consider a three-point function of scaling operators inserted at x_1, x_2, and x_3 with $x_1 < x_2 < x_3$ ($d = 1$) at a critical point. For simplicity suppose that $|x_1 - x_2| \ll |x_2 - x_3|$, then the RG will quickly bring operators 1 and 2 together to yield a factor of $|x_1 - x_2|^{-\Delta_1-\Delta_2}$. Operator 3 will also contribute a factor of $|x_1 - x_2|^{-\Delta_3}$ from the renormalization to the scale where x_1 and x_2 meet. The resulting composite operator made from 1 and 2 will in general be a sum of new scaling operators with different dimensions (in the continuum these are the operator product expansion coefficients). The dominant contribution will come from the operator with the lowest scaling dimension that has a nontrivial correlator with operator 3. Let the scaling dimension of that operator be Δ_{12}. We now renormalize further until x_3 and $x_2 \approx x_1$ come together, a process that gives additional factors of

$$\left(\frac{1}{|x_3 - x_2|/|x_2 - x_1|}\right)^{\Delta_{12}}, \tag{15}$$

and

$$\left(\frac{1}{|x_3 - x_2|/|x_2 - x_1|}\right)^{\Delta_3}. \tag{16}$$

The strange denominator appears because the separation between x_3 and $x_2 \approx x_1$ when x_2 and x_1 have been brought together is renormalized to $|x_3 - x_2|/|x_2 - x_1|$.

Setting $|x_2 - x_1| = \ell$ and $|x_3 - x_2| \approx |x_3 - x_1| = L$ we have

$$\langle O_1 O_2 O_3 \rangle \sim \frac{1}{\ell^{\Delta_1+\Delta_2}} \frac{1}{\ell^{\Delta_3}} \left(\frac{\ell}{L}\right)^{\Delta_{12}} \left(\frac{\ell}{L}\right)^{\Delta_3}. \tag{17}$$

Simplifying the right-hand side we find

$$\langle O_1 O_2 O_3 \rangle \sim \frac{1}{\ell^{\Delta_1+\Delta_2-\Delta_{12}}} \frac{1}{L^{\Delta_{12}+\Delta_3}}. \tag{18}$$

To compare to the conformal field theory result we must use the fact that a two-point function of scaling operators is only nonzero if the dimensions agree which requires $\Delta_{12} = \Delta_3$. Substituting our lengths into the expression in Eq. (14) gives the result

$$\langle O_1 O_2 O_3 \rangle \sim \frac{1}{\ell^{\Delta_1+\Delta_2-\Delta_3}} \frac{1}{L^{\Delta_2+\Delta_3-\Delta_1}} \frac{1}{L^{\Delta_1+\Delta_3-\Delta_2}}, \tag{19}$$

which perfectly reproduces our calculation using entanglement renormalization. It is interesting to note that entanglement renormalization is consistent with a slightly more general three-point function, a result we expect since entanglement renormalization can handle more general scale-invariant critical points without conformal symmetry. We can of course also consider even higher-point functions, but these are increasingly complex and not fixed by conformal invariance. Nevertheless, a similar analysis to that considered for the three-point function shows that the rough features of these correlation functions are reproduced.

VI. HOLOGRAPHIC DUALITY

The appearance of higher-dimensional black holes to describe thermal states of gauge theories is precisely the content of holographic gauge/gravity duality. The best known example is the duality between $\mathcal{N} = 4$ $SU(N)$ Yang-Mills theory in four dimensions, and a theory of quantum gravity, type IIB string theory, in a fluctuating spacetime that is asymptotically five-dimensional anti-de Sitter space times a sphere, $\mathrm{AdS}_5 \times \mathrm{S}^5$. When the field theory is strongly coupled and when the number N of "colors" tends to infinity, quantum gravity reduces to classical gravity in a weakly curved space.

In this limit, the $3 + 1$-dimensional gauge theory in infinite volume is dual to anti-de Sitter space in the Poincaré patch with metric

$$ds^2 = R^2\left(\frac{dr^2}{r^2} + \frac{-dt^2 + dx_3^2}{r^2}\right), \tag{20}$$

where again r represents length scale in the dual gauge theory. Finite temperature effects map to black hole physics in AdS and, in particular, thermal screening has an interpretation in terms of geodesics falling into the horizon. The entanglement entropy of a region A in the field theory is given by the area (in Planck units) of a minimal surface which hangs from the two-dimensional boundary of A into the bulk [26,27].

The general prescription in the holographic setting is to obtain field theory correlators by solving wave equations in the gravitational bulk as a function of certain boundary conditions. For scalar primary operators at a critical point, the dimension of the primary in the boundary field theory is related to the mass of a dual field in the gravitational bulk (the specific formula is $\Delta(\Delta - (d + 1)) = m^2 R^2$ for scalars). However, in a certain limit ($mR \to \infty$) the solution of the bulk wave equation is related to the trajectory of a massive particle in the gravitational spacetime. This is the so-called geometric optics approximation, and our computations of two- and three-point functions using entanglement renormalization are strongly reminiscent of this approximation. The fact that entanglement renormalization can reproduce correlation functions even when the dimension (bulk mass) is not large deserves further study.

In the case of $\mathcal{N} = 4$ $SU(N)$ Yang-Mills theory the constant R^3 measured in Planck units is proportional to N^2 and hence is indeed a measure of the number of degrees of freedom. A large value of N, where the geometry is weakly fluctuating in the quantum gravity theory, thus precisely corresponds to a highly entangled quantum system. From this perspective the main difference between the smooth geometry encountered here and the discrete geometry we constructed earlier is the amount of local entanglement, an observation that suggests a way to recover a smooth geometry from our lattice construction above by studying quantum systems with a large amount of local entanglement.

Because holographic minimal surfaces control entanglement we see that the metric of the bulk spacetime is intimately tied to entanglement, but the gravitational theory typically contains other fields which we must also define from field theory quantities. Consistent with the interpretation of the extra dimension in terms of scale, we can define the higher-dimensional bulk fields in terms of renormalized couplings in the dual field theory. The equations of motion for the bulk fields should be taken to be the renormalization group equations for the dual field theory [14]. One can check that relevant and irrelevant couplings in the Hamiltonian grow or decay as expected under entanglement renormalization [28]. We note in passing that there are additional issues away from large N i.e., defining fluctuating bulk fields, but we do not address these here.

One further interesting feature of gauge/gravity duality at finite temperature is that the geometry is not always equivalent to a black hole. For example, the entanglement structure of a gapped state should not change dramatically due to the presence of a small temperature. Alternatively, a conformal theory on a compact space can give at least two generic renormalization group behaviors based on whether one reaches zero spatial size or infinite temperature first. Something similar occurs in gauge/gravity duality in the form of the Hawking-Page transition [29]. If we perform entanglement renormalization on a compact system at finite temperature, we will reach a completely mixed state (black hole) before the whole system shrinks to a point only if the temperature is much greater than the inverse size of the system, so entanglement renormalization can reproduce a crossover version of the Hawking-Page transition. When a black hole does exist in the holographic geometry, the stretched horizon appears to be interpretable as the hydrodynamic scale in our construction, which is naturally distinct from the null surface horizon.

VII. DISCUSSION

We have described a framework for thinking about entanglement and correlation based on higher-dimensional geometry. We can construct an emergent holographic space from entanglement in a large class of many-body states including free bosons and fermions, quantum critical points, topological phases, frustrated quantum magnets, superconductors, and more. The gross features of entanglement and equal time correlation functions are encoded geometrically. This geometrical picture of entanglement is realized both in a concrete lattice setup based on entanglement renormalization and in the context of gauge/gravity duality, thus connecting these two beautiful ideas. The theory also incorporates black hole-like objects at finite temperature that seem to share many properties with more conventional black holes in semiclassical general relativity. We have not given a detailed proposal for the gravity dual of the Ising model, and if such a dual exists, it seems likely to be very complicated. Remarkably, much of this complexity seems irrelevant for the geometrical ideas explored here.

There are additional features as well as open questions. For simplicity, we worked primarily with the quantum Ising model in one spatial dimension, but the framework applies to more generic systems in higher dimensions. It is also possible to include time evolution, so that the fixed geometry found here is analogous to specifying the state in quantum gravity [30]. The inability to traverse wormholes is interpreted as the inability to use entanglement for faster-than-light communication. Other interesting geometries also exist, including situations where the effective spatial dimension changes as a function of scale or where the dynamical critical exponent flows. There are issues of nonuniqueness in the renormalization group that should be matched to bulk diffeomorphisms [31], and it must be possible to understand in what sense the geometry fluctuates away from large N.

Perhaps the most pressing issue for condensed matter applications is the need for a better understanding of what lies between gauge/gravity duality as inspiration and actually having the $\mathcal{N} = 4$ plasma in the lab. The framework outlined here seems well suited to attacking this question. For example, our construction applies to quantum $O(N)$-vector models, which are known to show hints of a holographic description [32]. A certain class of topological "string-net" phases realize exact versions of entanglement renormalization [33,34] and provide a useful testing ground. Finally, from the perspective of entanglement renormalization, variational principles for the higher-dimensional geometry may help simplify the search for quantum circuits to describe interesting many-body states. An important step towards making use of such variational principles is establishing more firmly the connections between entanglement renormalization and holography proposed here, and one simple way to make progress is to examine systems with many local degrees of freedom.

ACKNOWLEDGMENTS

I thank T. Lin, V. Kumar, N. Iqbal, D. Park, D. Vegh, T. Faulkner, K. Balasubramanian, T. Senthil, A. Adams, H. Liu, X.-G. Wen, L. Jones, G. Vidal, and S. Sachdev for comments. A special thanks to M. Barkeshli and J. McGreevy for enlightening discussions.

[1] D. C. Tsui, H. L. Stormer, and A. C. Gossard, Phys. Rev. Lett. **48**, 1559 (1982).
[2] R. B. Laughlin, Phys. Rev. Lett. **50**, 1395 (1983).
[3] X. G. Wen and Q. Niu, Phys. Rev. B **41**, 9377 (1990).
[4] A. Kitaev and J. Preskill, Phys. Rev. Lett. **96**, 110404 (2006).
[5] M. Levin and X.-G. Wen, Phys. Rev. Lett. **96**, 110405 (2006).

[6] G. Vidal, Phys. Rev. Lett. **99**, 220405 (2007).
[7] R. N. C. Pfeifer, G. Evenbly, and G. Vidal, Phys. Rev. A **79**, 040301 (2009).
[8] S. Montangero, M. Rizzi, V. Giovannetti, and R. Fazio (unpublished); Phys. Rev. B **80**, 113103 (2009).
[9] J. M. Maldecena, Adv. Theor. Math. Phys. **2**, 231 (1998).
[10] S. S. Gubser, I. R. Klebanov, and A. M. Polyakov, Phys. Lett. B **428**, 105 (1998).
[11] E. Witten, Adv. Theor. Math. Phys. **2**, 253 (1998).
[12] E. Alvarez and C. Gomez, Nucl. Phys. **B541**, 441 (1999).
[13] V. Balasubramanian, P. Kraus, A. Lawrence, and S. Trivedi, Phys. Rev. D **59**, 104021 (1999).
[14] J. de Boer, E. Verlinde, and H. Verlinde, J. High Energy Phys. 08 (2000) 003.
[15] G. Horowitz and J. Polchinski, arXiv:gr-qc/0602037v3.
[16] J. Eisert, M. Cramer, and M. B. Plenio, Rev. Mod. Phys. **82**, 277 (2010).
[17] C. Holzhey, F. Larsen, and F. Wilczek, Nucl. Phys. **B424**, 443 (1994).
[18] G. Vidal, J. I. Latorre, E. Rico, and A. Kitaev, Phys. Rev. Lett. **90**, 227902 (2003).
[19] S. Popescu, A. J. Short, and A. Winter, Nature Phys. **2**, 754 (2006).
[20] K. Wilson, Rev. Mod. Phys. **47**, 773 (1975).
[21] G. Vidal, Phys. Rev. Lett. **101**, 110501 (2008).
[22] L. Susskind, J. Math. Phys. (N.Y.) **36**, 6377 (1995).
[23] T. Jacobson, Phys. Rev. Lett. **75**, 1260 (1995).
[24] M. M. Wolf, F. Verstraete, M. B. Hastings, and J. I. Cirac, Phys. Rev. Lett. **100**, 070502 (2008).
[25] S. Sachdev, *Quantum Phase Transitions* (Cambridge University Press, Cambridge, 1999).
[26] S. Ryu and T. Takayanagi, Phys. Rev. Lett. **96**, 181602 (2006).
[27] D. Fursaev, J. High Energy Phys. 09 (2006) 018.
[28] G. Evenbly and G. Vidal, New J. Phys. **12**, 025007 (2010).
[29] E. Witten, Int. J. Mod. Phys. A **16**, 2747 (2001).
[30] A. Lawrence and A. Sever, J. High Energy Phys. 10 (2006) 013.
[31] V. Balasubramanian and P. Kraus, Phys. Rev. Lett. **83**, 3605 (1999).
[32] I. R. Klebanov and A. M. Polyakov, Phys. Lett. B **550**, 213 (2002).
[33] O. Buerschaper, M. Aguado, and G. Vidal, Phys. Rev. B **79**, 085119 (2009).
[34] Z. C. Gu, M. Levin, B. Swingle, and X. G. Wen, Phys. Rev. B **79**, 085118 (2009).